



Topoisomerase II β Gene Specific siRNA Delivery by Nanoparticles Prepared with c-ter Apotransferrin and its Effect on HIV-1 Replication

Lokeswara Bala Krishna Sunnam¹ · Anand K. Kondapi¹

Received: 21 February 2021 / Accepted: 5 May 2021 / Published online: 16 May 2021
© The Author(s), under exclusive licence to Springer Science+Business Media, LLC, part of Springer Nature 2021

Abstract

Topoisomerase II beta (Topo II β) is one of the two isoforms of type II topoisomerases present in higher eukaryotes. This 180 kDa nuclear protein involves in different cellular processes like transcription, recombination, etc., apart from its normal topological functions. Previously, we have reported the association of this isoform along with the other isoform topoisomerase II alpha (Topo II α) with HIV-1 reverse transcription complex and the downregulation of Topo II β expression resulted in incomplete reverse transcription. In this study, we have tested the Topo II β specific siRNA delivery using protein nanoparticles prepared with c-terminal domine of transferrin (c-ter) for the first time. Results show that, c-ter nanoparticles resemble apotransferrin nanoparticles in drug holding capability and drug delivery but with small in size. Topo II β specific siRNA delivered in the form of c-ter nanoformulation resulted in knockdown of Topo II β expression for the prolonged periods and which intern resulted in decreased viral replication of HIV-1.

Keywords Topoisomerase II β · Gene silencing · siRNA · HIV-1 · Apotransferrin · Nanoparticles

Introduction

Topoisomerase II beta (Topo II β) is one of the two so forms of Topoisomerase II with 180 kDa of weight. The expression of Topo II β was observed in all most all cells types of higher eukaryotes [1]. It is a nuclear localizing enzyme especially in the nucleoli and maintains study state level during different stages of cell cycle progression [2]. Topo II β has role in cellular differentiation [3], in different developmental stages and differentiation of neurons [4–6] including other non-proliferating and differentiated cells [7, 8] by regulating gene expression through chromatin remodeling. In induced differentiation studies on cultured cell models [9], it modulate genes responsible for reactive oxygen species regulation to maintain viability [10]. Topo II β has many interacting partners like p53, retinoblastoma protein, cAMP response element binding protein, c-jun, HDAC1&2, 14–3–3 ϵ and CAD

[11–18]. This vast range of interacting partners indicates role of this protein in diverged functions.

Several reports are available for the involvement of Topo II β in viral infections together with the other isoform of topoisomerase II called Topo II alpha which is having 170 kDa weight. These isoforms were reported in packaging of adenoviral genome and also in the expression of major late genes [19]. These isoforms were recruited at the site of Vaccinia virus replication in the cytoplasm of infected cells [20]. Early replicative stages of Moloney murine leukemia virus (MMLV) were impaired in the absence of the Topo II, which leads to decreased viral DNA synthesis and absence of viral genome integrations [21, 22]. In case of Human cytomegalovirus infections (HCMV) topo II inhibitors blocked viral DNA synthesis as well as viral replication [23, 24]. Like in other viruses, these isoforms have a crucial role in the HIV-1 replication [21, 25, 26]. Topo II activity was reported in proviral DNA synthesis and preintegration complex formation [27]. It was observed that, upon viral infection protein levels of both isoforms were upregulated but, Topo II β responded very early. siRNA mediated knockdown of these isoforms results in impaired reverse transcription [28].

Nanoformulation is one of the most effective method for delivery of therapeutic agents without altering their

✉ Lokeswara Bala Krishna Sunnam
lokeswarabks@gmail.com

¹ Laboratory of Molecular Therapeutics, Department of Biotechnology and Bioinformatics, School of Life Sciences, South Campus, University of Hyderabad, Prof. C. R. Rao Road, Gachibowli, Hyderabad 500049, Telangana, India

properties. The conversion of the therapeutic agents into nanoformulations may enhance the pharmacokinetic and pharmacodynamic properties [29]. The major goals in designing nanoparticles as a delivery system are particle size, surface properties and release of pharmacologically active agents site-specifically [30]. Even though several types of nanoformulations are available, based on the biodegradation/bioconversion of carrier material, protein nanoparticles have additional advantage. Using ligands in nanoformulations we can attain delivery of the compounds to the required cells or organs which has expression of ligand specific receptor. One of such nanoformulation is transferrin nanoparticles.

Transferrin (Tf) is a serum abundant protein involved in Iron (Fe) transportation to the cells by binding to the transferrin receptor (Tfr) expressed on the cell surface. The Tf-Tfr mechanism of iron transportation was well established. Once the Tf-Tfr complex is formed, it gets internalized to cytosol and forms endosome. The ATP-dependent proton pump present on the surface of the endosome pumps H^+ ions into endosome resulted in reduced pH. Under low pH (5.5) conditions, conformational changes of Tf takes place to enable Iron release [31]. Later the endosome fused with the cell membrane to expose Tf-Tfr complex which leads to the complex dissociation and this is a cyclic process [32]. Many studies have used Tfr as target for delivery of various therapeutic agents by preparing nanoformulations using its ligand Tf, antibodies or antibody fragment specific for Tfr extracellular domain as carrier proteins [33] and exploited this Tf-TFR mechanism for site specific delivery of various therapeutic metal ions, drugs, proteins and genes [34].

In this current study, we prepared nanoparticles using c-terminal lobe of TF (c-ter nano) and tested the siRNA delivering capability of these nanoformulation. Using these nanoparticles we demonstrated successfully the impaired replication of HIV-1 virus by downregulating Topo II β protein expression.

Materials and Methods

Cell and Virus Culture

SupT1 [35] cells used for viral propagation and infection experiments were cultured in RPMI-1640 (Gibco-BRL, Invitrogen, CA, USA) medium with 10% FBS (Gibco-BRL). HepG2 and HeLa (NCCS-Pune) were cultured in DMEM (Gibco) with 10% FBS (Gibco). All of these cells were maintained at 37 °C in a humidified CO₂ incubator (Thermo Scientific) with 5% CO₂ concentration. For virus production, SupT1 cells (0.1 millions) were infected with viral stock (10 ng) of HIV-1 93IN101 (subtype C) in the presence of 8 μ g/ml Polybrene (Sigma, St. Louis, MO, USA) overnight. These infected

cells were washed thrice with 0.1 M phosphate buffered saline (PBS) and seeded back in complete medium. 96 h later the replicated virus in cell culture media was estimated with p24 ELISA kit (ABL Inc, Kensington, MD, USA). The cell culture supernatant containing virus was filtered using 0.45 μ membrane filter (Pall Corporation, USA) and used for infection experiments.

Viral Infections

In infection studies, 5×10^6 cells were infected with HIV-1 as protocol published [28] and collected at 0, 4, 12 and 24 h of post infection. In all infection experiments 20 ng (p24 quantity) of virus for every 2×10^6 cells (100 MOI) were used in serum free media in presence of Polybrene (8 μ g/ml). For experiments where cells were used at later time points, i.e., > 6 h of post infection, 10% serum was added.

Receptor Level Analysis

$1-2 \times 10^6$ cells of infected and control SupT1 cells were washed thrice with cold PBS and were incubated on ice with 1:100 diluted mouse anti-Transferrin receptor monoclonal antibody (TfR/CD 71) (Santa Cruz Biotechnology, Inc) for 60 min., later cells were washed with ice cold PBS and incubated in 4% PFA for 30 min on ice. After washing, cells were incubated for 1 h at room temperature with 1:2000 anti-mouse secondary antibody labeled with FITC (Santa Cruz Biotechnology, Inc), washed and counter stained with Propidium Iodide (PI) (Invitrogen). Cells were analyzed in CyFlow space flow cytometer (PARTEC, GmbH, Germany).

Cloning of C-ter Lobe of Apotransferrin

Total RNA was isolated from HepG2 cells using TRI reagent (Sigma). cDNA was synthesized using SuperScript-III reverse transcription kit (Invitrogen). C-ter of Tf ORF (from 1081 to 2061 bp of GenBank: M12530) was amplified using primer (Table 1) and Dreamtaq master mix (Fermentas). 95 °C for 2 min, 94 °C for 30 s, 55 °C for 30 s, 72 °C for 1 min, for 35 cycles and finally 72 °C for 5 min are the PCR conditions. The amplicons were gel purified (Gel extraction kit-Qiagen) and cloned into pDualGC vector (stratagene) using Eam1104I (Fermentas). *E. Coli* strain (DH5- α) was used for the transformation of ligate and recombinant plasmid was propagated after confirmation by PCR, restriction enzyme digestion and sequencing (Eurofins). *E. Coli* strain (BL21: DE3-Lac-I) was used for protein expression.

Table 1 Sequence of the oligomers used in this study

S. No.	Primer	Sense strand/Forward primer 5'–3'	Antisense strand/Reverse primer 5'–3'	Purpose
1	c-ter	ATGGTGAAGTGGTGTGCGCTGAGCCAC	AAGTCTACGGAAAGTGCAGGCT	Tf c-ter lobe amplification
2	Topo II β -siRNA	GCTTAACAATCAAGCCCGTTT	ACGGGCTTGATTGTTAAGCTT	Topo II β knockdown
3	T7 promoter	TAATACGACTCACTATAG	ATTATGCTGAGTGATATC	Synthesis of siRNA
4	GFP siRNA	ATGAACTTCAGGGTCAGCTTG	CGGCAAGCTGACCCTGAAGTTC	siRNA control

From top to bottom 1—Used for the amplification of the c-terminal region of the apotransferrin cDNA from HepG2 cells. 2—siRNA sequence used for the knockdown of Topo II β expression. 3—T7-Promoter sequence for siRNA synthesis. 4—Green fluorescent protein specific siRNA sequence as a control

Overexpression of C-ter Lobe of Apotransferrin Protein

Recombinant plasmid harboring E.Coli-BL-21: DE3-Lac-I were cultured to a OD 600 = ~0.45 and induced for protein expression with various concentrations of isopropyl β -D-1-thiogalactopyranoside (IPTG) (Fermentas) for different time periods in an orbital shaker at 450 rpm and 37 °C. Cells were harvested at mentioned time periods and analyzed using 10% SDS-PAGE.

Recombinant Protein Purification

E. Coli cells from 100 ml culture was harvested and lysed in 10 ml lysis buffer (50 mM glucose, 25 mM Tris–Cl, 10 mM EDTA and pH 7.3) by sonication. Cell lysate was centrifuged at 2000 rpm for 5 min and supernatant was collected. Proteins were fractionated using ammonium sulfate (AS) method. At 4 °C, 20% (1.13 gm/10 ml) AS was added, stirred for 30 min then centrifuged at 12,000 rpm for 10 min. The pellet was collected and dissolved in 1 ml of lysis buffer. The same step was repeated with 30% salt (0.59 gm) and 40% salt (0.61 gm) of AS. All the pellets were dialysed in 1 l each of phosphate buffer saline (PBS) at 4 °C. PBS was changed with fresh PBS after 2 h and dialysed for overnight and were concentrated on sucrose. The concentrates were subjected to Size exclusion chromatography (SEC) using 150 cm column packed with Sepharose CL 6B (Amersham). Before applying the sample, the column was equilibrated with at least two column volumes of the PBS until the baseline is stable. Sample equal to 2% of the total bed volume was applied and 1 ml fractions were collected and analyzed on SDS-PAGE with silver staining. Protein concentration was determined and stored in – 70 °C deep freezer (Sanyo).

Silver Staining

The SDS-PAGE gels were fixed in fixing solution (40% methanol, 5% formaldehyde) for 10 min. and washed the gel twice in water each time 5 min. then gel was soaked in sodium thiosulfate solution (0.02% Na₂S₂O₃) for 1 min.

and rinsed with water twice for 20 s each. Then the gel was soaked in silver nitrate solution (0.1% AgNO₃) for 10 min. after rinsing once with water and once with a small volume of developing solution (3% Na₂CO₃, 0.02% formaldehyde, 0.00002% Na₂S₂O₃), gel was soaked in developing solution till the bands were appeared and the reaction was stopped with stop solution (2.3 M citric acid). For Nucleic acid staining, For 5 min the gels were soaked in fixing solution (10% absolute ethanol, 0.5% acetic acid), shifted to Impregnation solution (0.15% AgNO₃, 2 ml 37% HCOH) and soaked for 6–7 min. Later gels were rinsed 10–20 s with distilled water and soaked in developing solution (1.5% NaOH, 3 ml 37% HCOH) until the bands appear. Once the bands reaches optimal intensity, development was stopped by incubating the gels for minimum 2 min in stop solution (10% absolute ethanol, 0.5% acetic acid).

siRNA Synthesis and Transfection

Topo II β specific siRNA was synthesized by following the protocol as published earlier [28, 36]. Briefly, T7 promoter oligo was annealed with 1 nM of each siRNA oligos (sequences 1–3, Table 1). The transcription was performed in 50 μ l of transcription buffer (40 mM Tris– HCl pH 7.9, 6 mM MgCl₂, 10 mM DTT, 10 mM NaCl and 2 mM spermidine), 1 mM rNTPs, 0.1 U yeast pyrophosphatase, 40 U RNaseout and 100 U T7 RNA polymerase containing 200 pM of the template. Reaction was carried by incubating the mixture for 2 h at 37 °C, and DNA templates were removed by digesting with 1 U DNase I at 37 °C for 15 min. Synthesized sense and antisense RNAs were mixed in equal ratio and heated to 95 °C for 5 min followed by 1 h at 37 °C for annealing. The ds-siRNA was precipitated with 0.2 M sodium acetate pH 5.2 and 2.5 vol. of ethanol. The obtained pellet was washed once with 70% ethanol, dried and suspended in 50 μ l of water. In transfection procedure, ~0.2 μ M siRNA/ 1 \times 10⁶ SupT1 cells were used. GFP siRNA used as negative control at 48 h post-transfection, cells were analyzed for target protein knockdown by Western blot.

Preparation of Protein Nanoparticles

Protein nanoparticles were prepared according to the procedure described previously [37] with slight modifications. 350 µg of r-ctf of aTf (protein) was mixed with 10 µl drug (100 mM stock/50 mg/ml) or siRNA (200 nM) then total volume was made up to 260 µl with PBS (0.1 M, pH 7.4) and incubated on ice for 30 min. To the mixture, 1 ml of olive oil at 4 °C was added by mixing slowly. The sample was sonicated at 4 °C using amplitude 50 Amps, 3 × 5 min. pulses- 30 s on and 30 s off with an interval of 1 min every 5 min in sonicator (300 V/T, Biologics Inc., Manassas, Virginia, USA). The resulting mixture was immediately frozen in liquid nitrogen and transferred to ice and incubated for 4 h to overnight. After thawing, the particles formed were pelleted by centrifugation at 8000 rpm for 15 min and the pellet was extensively washed with diethyl ether and dispersed in 1 ml PBS and stored at 4 °C.

Field Emission Scanning Electron Microscopy (FESEM) Analysis

Structure and morphology of the nanoparticles were investigated using scanning electron microscope (Philips FEI-XL 30 ESEM, USA—operated at 20 kV); manufacturer's instructions were followed for sample preparation, i.e., nanoparticles were dried on a clean 5 × 5 mm glass piece and dried overnight in sterile conditions. After completion of processing, scanning samples followed by data collection and analysis of data. Pictures of nanoparticles were captured and size was estimated.

Estimation of Encapsulated Doxorubicin

The leftover Doxorubicin in Aqueous phases was estimated by taking 5 µl of each sample and diluted to 40-fold. The fluorescence of the drug was measured at 490 nm wave length with a UV–Vis spectrophotometer (Jasco V550). We have used olive oil and PBS as blanks. Based on these values, the total amount of leftover drug was calculated based on the standard graph plotted using different concentrations of Doxorubicin. The amount of drug leftover (WF) was subtracted from the total amount of drug (WT) used in the preparation to get the amount of drug encapsulated (WE). The experiment was done in triplicates and the results were plotted.

The encapsulation efficiency (EE %) was calculated using $WE/WT \times 100$.

pH-Dependent Release of Doxorubicin

Nanoparticles were suspended at the rate of 5 µl/200 µl of 0.1 M PBS with various pH (2, 5.5, 7.4 and 9) conditions and incubated for different time points (0, 1, 2, 4 and 6 h).

After incubation the volume of PBS was increased to 2 ml by adding 1.8 ml of PBS, centrifuged at 12,000 rpm for 15 min at 4 °C. The amount of drug released was estimated as mentioned above. Experiment was repeated three times and the results are presented in terms of mean and standard deviation.

Delivery of Doxorubicin into the Cells

HeLa cells were grown on cover slips at the density of 1.5–2 million/ml of the culture media in 24 well plate. Before 1 h to the addition of the drug, media was changed with fresh media. Equal amount of drug and nanodrug were added to separate wells and incubated for 0, 1 and 2 h. Later cells were washed thrice with ice cold 1 × PBS and fixed the cells with 4% paraformaldehyde at room temperature for 10 min. Cells were stained with DAPI and were photographed in Zeiss LSM 710 confocal microscopy at 630 × oil emulsion at wave lengths 557/576 nm and 360 nm respectively for drug and DAPI.

siRNA Loading Capacity of c-ter Nanoparticles

siRNA was extracted from 100 µl of nanoparticles using TRI reagent. The pellet obtained was dissolved in the 30 µl Milli-Q water and mixed with 10 µl of 4 × gel loading dye and loaded without boiling on the 12% SDS-PAGE and gels were silver stained. The obtained band intensities were measured using Image J software (NIH) and back calculated with known concentration 20 ng siRNA loading control to determine the siRNA concentration in nanoparticles in terms of percentage (%).

Cytotoxicity Assay (MTT Assay)

4×10^5 cells/well SupT1 cells transfected with siRNA either in nanoform or Lipofectamine 2000 (Invitrogen, CA, USA) separately in the presence or absence of penicillin (100 units/ml) and streptomycin (100 mg/ml) (Gibco-BRL, Invitrogen, CA, USA). seeded in 96 well tissue culture plate (Orange Scientific) in 200 µl complete media were incubated for 16 h. Thereafter, the plate was spun and the supernatant (mixture of media and inhibitor) was removed. 20 µl MTT (5 mg/ml) along with 180 µl complete media was added and incubated for 4–8 h. The cells were then pelleted on centrifugation at 1000 rpm for 10 min and supernatant (media) was removed. 200 µl of DMSO or acidic isopropanol was added and left at room temperature for 5–10 min. The absorbance is recorded at 570 nm using a plate reader.

Cell Extracts Preparation and Western Blot

From siRNA-treated and untreated cells, total protein was prepared by following protocol published earlier [28]. Cells were lysed in protein extraction buffer containing [10 mM Tris–Cl (pH 7.4), 0.1% Triton X-100, 1 mM PMSF, 1 mM EDTA and 1 mM DTT] for 10 min on ice with protease inhibitor cocktail (GE Healthcare, UK). The lysates were centrifuged for 15 min at 4 °C at 12,000 g. The collected supernatants were quantified by Bradford method. 100 µg of protein from each samples was subjected to SDS–PAGE (10%) in Tris–glycine buffer and the resolved peptides were Electro-blotted on nitrocellulose membrane (NCM) (Pall) using the Trans-Blot (Bio-Rad, Hercules, CA, USA) by following Towbin et al. [38]. The NCM was blocked with 3% BSA (w/v) in Tris-buffered saline (TBS) [10 mM Tris–Cl (pH 7.4), 150 mM NaCl and 0.1% Tween-20 (0.1% v/v)] for 1 h at room temperature followed by washing with TBST (TBS containing Tween-20 (0.1% v/v)). The NCM was probed with mouse anti-human Topo IIb (BD Biosciences, USA) (1:1000 dilution) for overnight at 4 °C. After three washes with TBST, the blot was incubated with HRP (horseradish peroxidase) conjugated goat antimouse IgG secondary antibody (1:5000 dilution) (Millipore, MA, USA) for 1 h at room temperature on rocker. After washing with TBST, blots were then developed with ECL substrate (Thermo Scientific, USA) and chemiluminescence was captured by exposure to X-ray film (Kodak, USA).

HIV-1 p24 Antigen Assay

Viral replication was estimated by measuring the p24 antigen present in the cell culture supernatant of infected cells. After 96 hpi, viral p24 protein with p24 ELISA kit following the manufacturer's instructions. Briefly, in each ELISA plate well, 25 µl of the disruption buffer was distributed. To these wells 100 µl of cell culture supernatant was added and incubated at 37 °C. After 1 h, these wells were washed thrice with 1X wash buffer. Then 100 µl of anti-p24 peroxidase-conjugated antibody was added and incubated at 37 °C for 1 h. ELISA plate wells were washed as mentioned above, and to each well, 100 µl of peroxidase substrate was added and incubated in dark at room temperature. After 20 min, reaction was stopped by addition of 100 µl stop solution and the color intensity was measured at 450 nm. Un-infected cell culture supernatant was used as negative control.

Densitometry Analysis

Densitometry analysis was done using ImageJ 1.46r software developed by NIH, USA.

Statistical Analysis

Data were presented as mean \pm SEM (standard error of mean). Number of samples/repeats for each experiment/assay is indicated in the legends to figures. Differences between groups were evaluated using Student's t test or one-way analysis of variance (ANOVA) with Turkey's post hoc analysis. For each test, * indicates significance at $p \leq 0.05$, ** indicates significance at $p \leq 0.01$.

Results

Analysis of Transferrin Receptor (TfR) Levels

SupT1 cells were infected with HIV-1 and samples were collected at different time points to analyze the effect of HIV-1 infection on TfR levels which were present on the activated cell surface using flow cytometry. Results (Fig. 1a) indicated that, the area under 0 h of post infection (hpi) represent study state level of TfR expression on SupT1 cells. At 4 hpi, even though non-significant, a slight increase was observed in receptor levels. At 12 hpi, a different receptor levels and different populations were observed. It shows the effect of HIV-1 infection on degradation of TfR may be taking place around this time point. The overall decrease in receptor levels observed in terms of intensity was a significant decrease. This degradation process continued further to 24 hpi which is the last time point in this study. At 24 hpi, the decrease was observed in the maximum population which represent by a peak shift toward left side. The mean intensity at 0, 12 and 24 hpi was at around 125, 109 and 93 units respectively represents the gradual decrease of cell surface TfR levels and there is no sudden drop in receptor levels.

Cloning of C-Terminal (rec. C-ter.) Apotransferrin

Results showing (Fig. 1b) success full amplification of the C-ter 1 kb region of the transferrin ORF from total RNA isolated from the HepG2 cell line. The amplicon was cloned into a pDual GC vector (Fig. 1c) which can facilitate the overexpression of the cloned DNA fragment in both mammalian and E.Coli expression systems (dual expression vector) between two restriction sites of Eam1104I enable the recombinant fusion protein with His tag (Fig. 1c). The ligated product was transformed into competent DH5 α E. Coli cells. The prominent colonies appeared on kanamycin selection media were analyzed for the presence of recombinant plasmid which was confirmed by PCR and further re-conformed by restriction enzymatic digestion with Eam1104I (Fig. 1c) showing successful release of the cloned 1 kb DNA fragment by leaving 5.7 kb vector backbone from the recombinant plasmid.

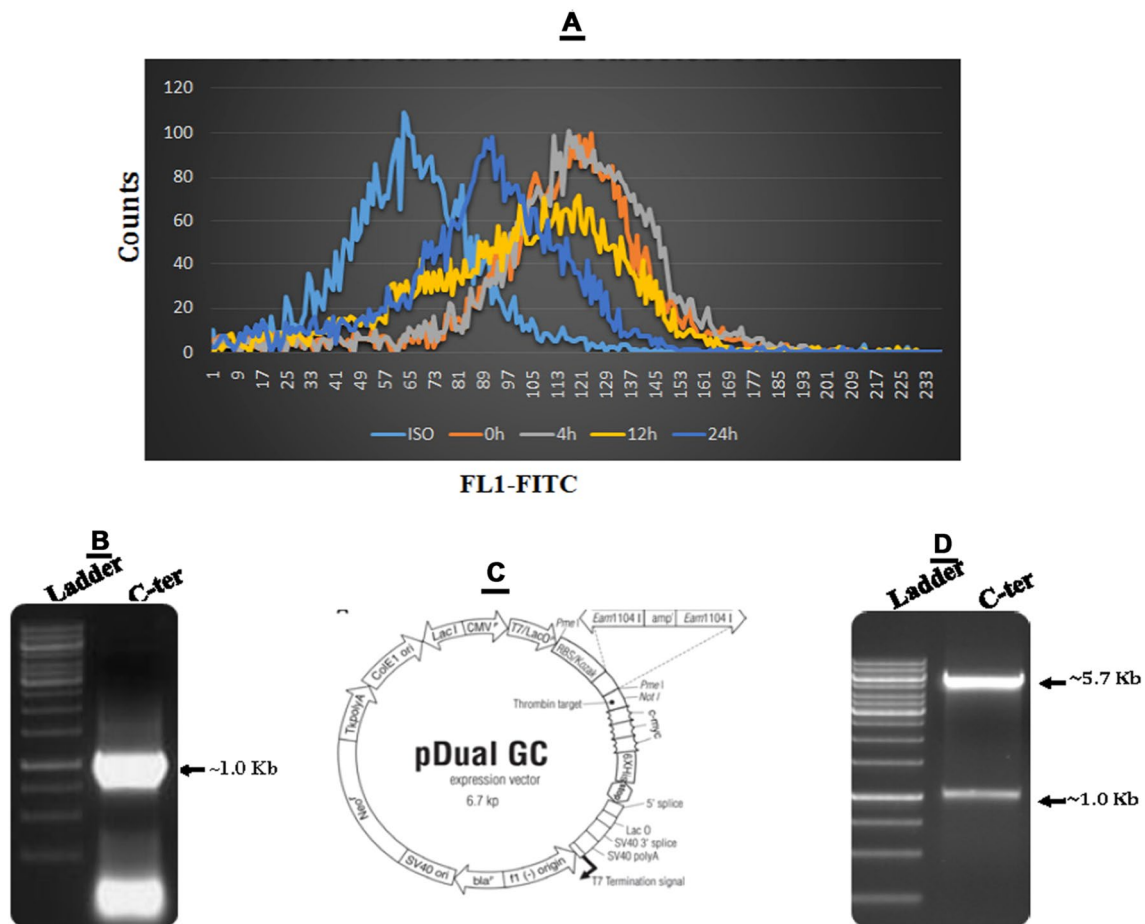


Fig. 1 Analysis of transferrin receptor expression in post infected cells and cloning of C-ter lobe of human apotransferrin. The **a** of above figure (Fig. 1) represent the dynamics of transferrin receptor upon HIV-1 infection. Blue color: isotopic control, Orange: 0 h of post infection, Ash: 4 h of post infection, Yellow: 12 h of post infection and Dark blue: 24 h of post infection. The obtained intensities were plotted as counts vs intensities. **b** represent the amplification

of the C-ter region of transferrin. Lane one: 10 Kb ladder, lane two: amplified product of the transferrin C-ter region. **c** represent the schematic diagram of the expression vector pDual GC.; **d** represent the conformational steps of cloning (release of the insert). Lane-1 10 Kb ladder, lane-2 vector backbone of 5.7 Kb and 1 Kb insert (from top to bottom) (Color figure online)

Expression of the rec. C-ter Transferrin in *E. Coli* BL21 (DE3-Lac-I)

After confirmation of pDual GC harboring C-ter region of the human transferrin, the recombinant plasmid was transformed to *E. Coli* BL21 (DE3-Lac-I) and PCR positive colonies were selected from kanamycin selection agar plate. Selected single colony was cultured in LB broth and titrated for the effective IPTG concentration (Fig. 2a). Results showed a good quantity of overexpression ~ 45 kDa position with 1 mM concentration of IPTG and the time of incubation (data not shown) to get the optimal expression of rec. protein was found to be 4 h. Samples were further analyzed for the presence of

the recombinant protein expressed (Fig. 2b) by western analysis using poly-Histidine antibody confirmed the over expression of the ~ 45 kDa rec. protein (Fig. 2b) based on the presence of the poly-Histidine in the rec. protein which is a vector property.

Purification of rec. Ctd of Tf.

Proteins in the crude *E. Coli* cell lysate were precipitated with mentioned percentages of Ammonium sulfate $((\text{NH}_4)_2\text{SO}_4)$ and a small fractions of the resulting protein pellets were boiled in 1XSDS loading buffer and analyzed in 10% SDS-PAGE (Fig. 2c) showing the precipitation of the maximum amount of ~45 kDa protein in 20% ammonium

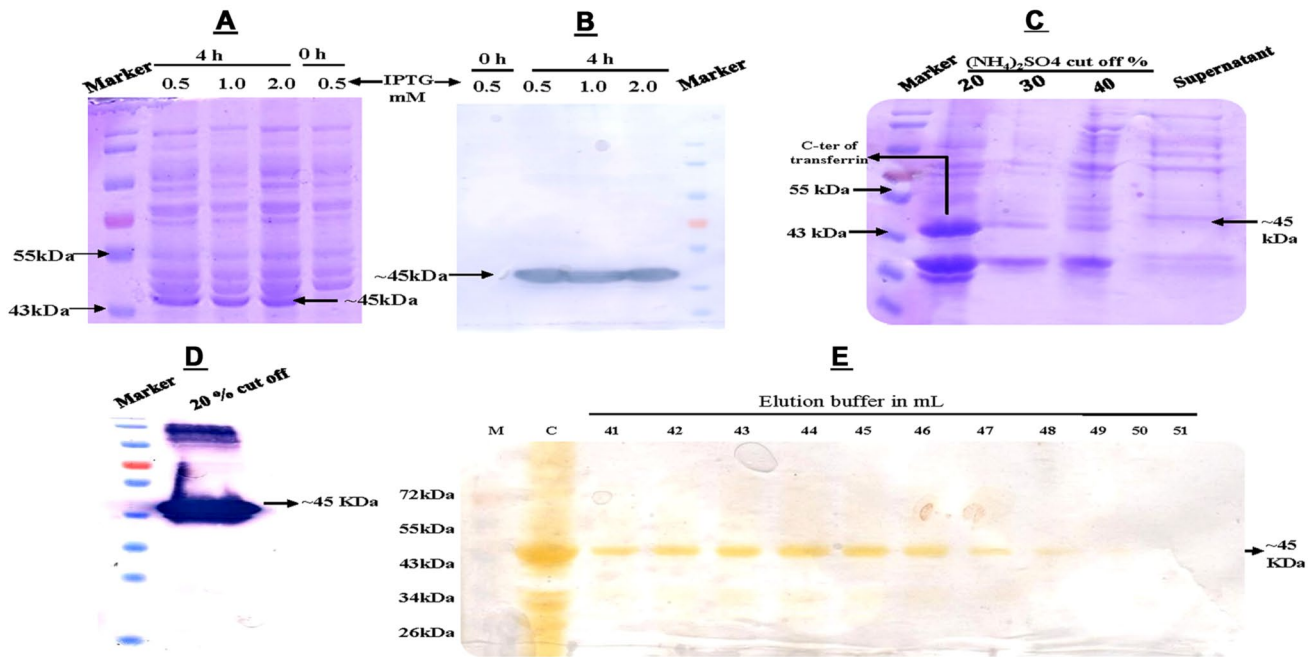


Fig. 2 Expression and purification of transferrin c-terminal lobe. **a** the coomassie stained gel representing the overexpression of the C-ter lobe of transferrin in response to IPTG. Column 1–5 (from left to right) represent the protein marker, 0.5, 1.0, 2.0 and 0.5 M concentrations of IPTG used and the induction period was for 4 h. Column 2–4 represent the protein expression from recombinant plasmid. Column 5 represent the empty vector control. **b** western blot of the overexpressed protein. Column 1–5 (from left to right) represent the 0.5, 2.0, 1.0, 0.5 M of IPTG induction for 4 h. Column 2–4 represent the protein from recombinant plasmid. Column 1 represent the protein from empty vector control and column 5 represent protein marker. **c**

ammonium sulfate precipitation of the rec. protein. Mentioned concentration of ammonium sulfate was added to cell lysate and the precipitated proteins were analyzed on coomassie stained SDS-PAGE. Extreme left protein ladder and extreme right supernatant after 40% precipitate removal. **d** western blot confirmation of rec. protein in 20% ammonium sulfate precipitate. **e** represent the silver stained SDS-PAGE of different fractions from size exclusion chromatography. M-Protein marker, C-crude 20% precipitate as control, 41–51 are the fractions of elute and 41–48 are the fractions of elute containing protein

sulfate concentration along with other proteins. The absence of this ~45 kDa protein was observed in pellets with 30–40% of ammonium sulfate and also in the final resulting supernatant. Western blot analysis with poly-Histidine antibody confirm the presence of the of rec. protein in the precipitate from 20% Ammonium sulfate concentration (Fig. 2d). These results confirm the precipitation of the major part of the rec. protein with 20% ((NH₄)₂SO₄) concentration. The rec. Ctd of Tf from the 20% ammonium sulfate pellet was further purified by size exclusion chromatography (SEC) to eliminate the co-precipitated proteins. Eluted buffer was collected at 1 ml volumes and tested for the presence of protein by 10% SDS-PAGE and silver staining. Results show that these elutes from 41 to 48 (Fig. 2e) are having the ~45 kDa rec. protein without any other proteins as contaminants. These eight elutes were pooled, concentrated and stored at –70 °C for further use.

FESEM Analysis of rec. Ctd Nanoparticles

Nanoparticles prepared using c-ter Tf and native Tf were tested for the shape and size by FESEM analysis. Nanoparticles from both preparations were spread and dried on 0.5 × 1.0 cm piece of microscopic glass slide separately, processed and subjected to FESEM. The data (Fig. 3) obtained from FESEM analysis clearly represented the shape of the nanoparticles were size of them were calculated. From both preparations the shape of the nanoparticles were found to be spherical (Fig. 3a, b). There was no effect of the size of the protein on the shape of the nanoparticles prepared in this study. But in the case of size, even though different size populations were observed in nanoparticles prepared with c-ter Tf protein, the average size of the nanoparticles were ~25 nm (nm) (Fig. 3b). In the preparation of nanoparticles using native Tf, the average size was found to be ~70 nm (Fig. 3a). In this study we found that decrease in the size of carrier protein resulted in small size nanoparticles.

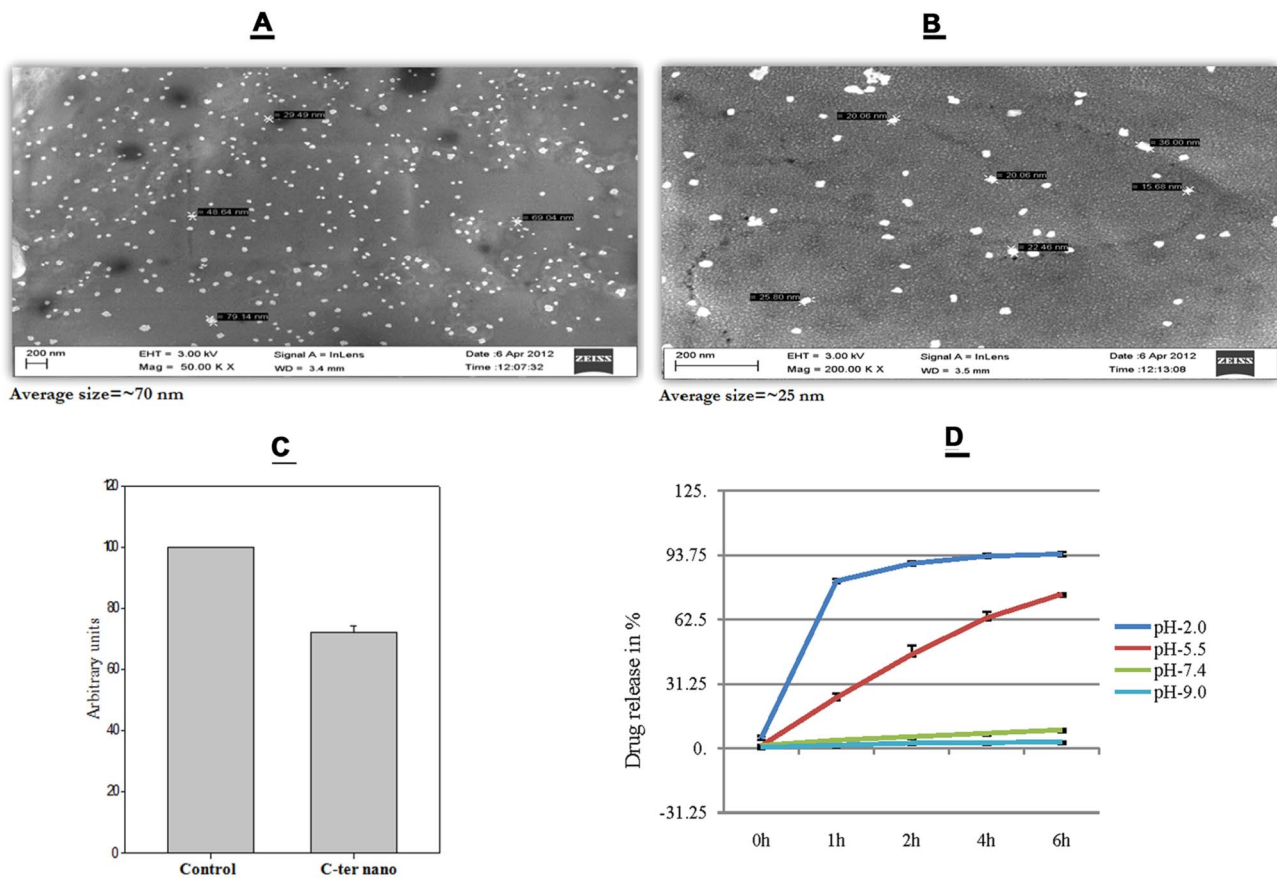


Fig. 3 Characterization of c-ter nanoparticles. **a** represent the FESEM photograph of doxorubicin loaded nanoparticles prepared with whole apotransferrin. The average size of the particles was ~70 nm. **b** represent the FESEM photograph of doxorubicin loaded nanoparticles prepared with the rec. c-terminal apotransferrin. The average size of the particles was ~25 nm. **c** comparative analysis of the doxorubicin fluorescence intensity measured at 490 nm. Control represent the free doxorubicin used in nanoparticles preparation. C-ter nanorepresent

the amount of drug encapsulated in nanoparticles. **d** represent the pH-dependent release of the drug from nanoparticles prepared with rec. apotransferrin. Blue:pH 2.0, Red:pH 5.5, Green and Cyan: pH 7.4 and 9.0 respectively. Obtained fluorescent intensities in % were compared with known concentration of free drug and plotted. **c–d** are the mean values of three independent experiments with standard error (MEAN + SE) (Color figure online)

Drug Holding Capacity of Nanoparticles

Synthesis of small-sized nanoparticles raises a question on the efficiency of their drug holding capacity. After preparation of C-ter nanoparticles with drug, we have evaluated the amount of drug present in the nanoparticles by extracting the drug from a small portion of nanoparticles by incubating them in pH 7.4 PBS for overnight. The drug released into the buffer was estimated by reading OD at 490 nm and compared against the standard concentrations. The amount of drug present in total nanoparticles was calculated in percent and plotted (Fig. 3c). Result shows that the C-ter nanoparticles could able to retain approximately 72% of the drug input. We observed the

loss of drug in three ways from the preparation. Some amount of drug retention was observed in oil phase. Very little amount of drug retention was found in buffer phase and some loss of drug found during washing of the nanoparticles with PBS. Further analysis shows the rec. Ctd nanoparticles may not allowed diffusion of drug into PBS. Whatever the little drug observed in the PBS, maybe the drug adsorbed on the outer surface of the nanoparticles. These results show the nanoparticles made of c-ter Tf may have 72% drug holding capacity.

Effect of pH on Drug Release from rec. Ctd Nanoparticles

Drug release from the c-ter Tf nanoparticles in response to various pH conditions were studied under different incubation times. C-ter Tf nanoparticles were incubated in PBS of pH 2.0, 5.5, 7.4 and 9.0 for 0–6 h. in triplicates and the amount of drug released from each sample was measured (Fig. 3d). These nanoparticles in response to pH 2.0 in drug releasing showed a log phase from 0 to 1 h of post incubation. At later time points there was no much change in drug release represented a stationary phase. There was a slow and study drug release was observed from these nanoparticles at pH 5.5. The drug release pattern from 0 to 6 hpi represented a log phage without stationary phage. At pH 7.4 release of drug from nanoparticles was not observed. Similar kind of result observed at pH 9.0 also. These results represent the requirement of acidic environment for the release of the drug from c-ter Tf nanoparticles. Especially around pH 5.5, the drug release was steady for long periods. The alkaline environment could not stimulate the drug release.

C-ter Tf Nanoparticles Mediated Drug Delivery

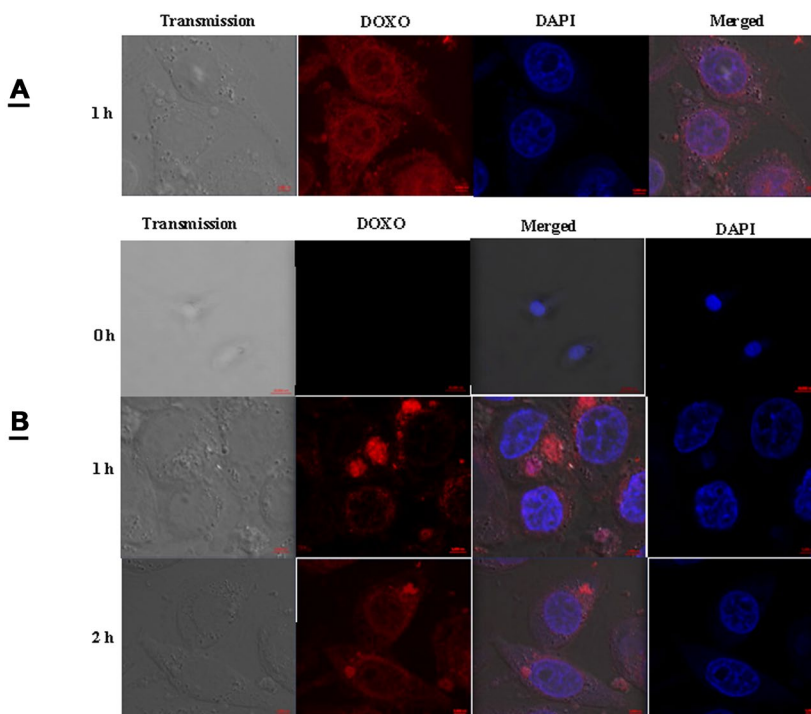
To evaluate the efficacy of the c-ter nanoparticles in drug delivery to the HeLa cells in vitro, doxorubicin loaded nanoparticles were prepared and tested. HeLa cells were grown on the microscopic cover slips and incubated with nanoparticles for 0, 1 and 2 h. After each mentioned time period, samples were collected processed and examined under confocal

microscope, images were taken and analyzed. As a control, cells were treated with direct drug (Fig. 4a). Results show that in the nanoparticles treated cells, at 1 h of post incubation, nanoparticles were accumulated on the cell wall and very little amount of drug entered into cells. But at 2 h of post incubation (Fig. 4b), more amount of drug spread in the cytoplasm and fewer amounts observed in the nucleus and also the accumulation of drug on the nuclear membrane was also observed. It shows that controlled release of the drug from the nanoparticles. In contrast to this, in cells treated with direct drug (Fig. 4a), at 1 h of post incubation the drug spread evenly in the cytoplasm and nucleus but little bit more amounts was observed at the nuclear membrane. It shows that drug directly diffused through the cell.

siRNA Holding Capacity of Nanoparticles

Nanoparticles were synthesized for the delivery of siRNA was analyzed for the siRNA holding capacity. siRNA from a fraction (1/10) of nanoparticles was extracted and run on 12% SDS-PAGE and silver stained. The obtained bands intensities were measured and concentration was calculated with reference to control (20 ng siRNA in lane-3 Fig. 5a). And found that it is approximately 16 ng (lane 4. Fig. 5a). The back calculation show that the siRNA available in the total nanoparticles preparation was only 160 ng In terms of percent calculation, it shows approximately 80% (Fig. 5b). The analysis of cytotoxicity during siRNA transfection (Fig. 5c) revealed the lesser cytotoxicity in nanotransfection than lipofectamine 2000 show the safety of nano-siRNA

Fig. 4 c-ter nanoparticles mediated delivery of Doxorubicin in cells. The figure representing the difference between the Doxorubicin entry into cultured HeLa cells. **a** represent the accumulation of the free doxo into the HeLa cells after 1 h of post incubation. DOXO- doxorubicin and DAPI- nuclear stain to visualize nucleus. **b** represent nanodoxo delivery. Cells were observed at 0, 1 and 2 h of post incubation. The Red color in cells represent the accumulated doxorubicin and the blue color represent the DAPI (Color figure online)



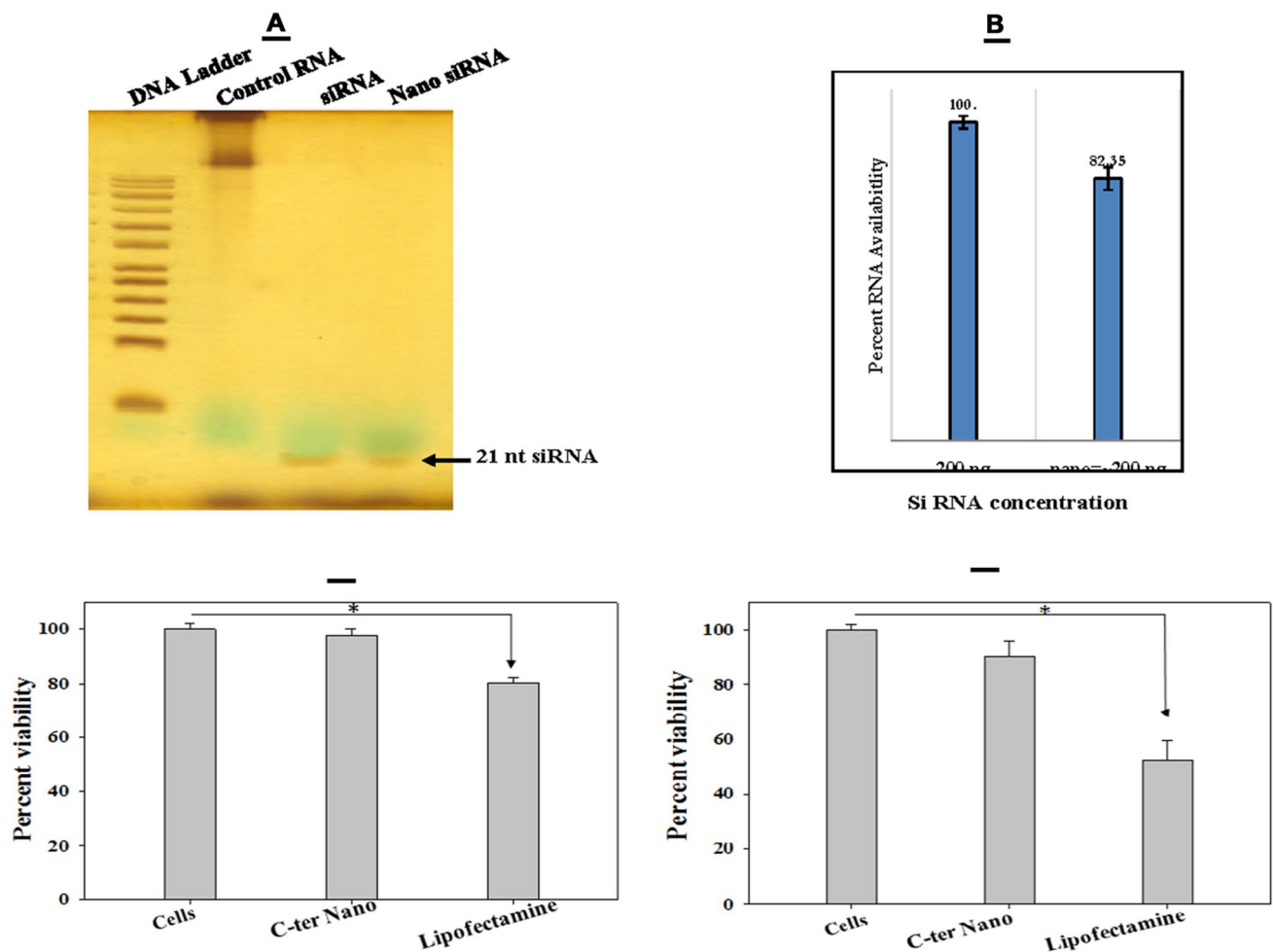


Fig. 5 siRNA loading capacity and cytotoxicity. **a** The silver stained SDS-PAGE gel showing the amount of siRNA present in 100 μ l of nanoparticles. From left to right, lane 1: DNA ladder, lane-2: total RNA isolated from SupT1 cells loaded as RNA control, lane-3: 20 ng of siRNA loaded as known concentration control. Lane-4: siRNA extracted from 100 μ l of nanoparticles. **b** siRNA loading efficiency of nanoparticles. Densitometry analysis of siRNA present in 100 μ l of siRNA nanoparticles in comparison to the total input siRNA (200 nM). **c** Cytotoxicity exerted by siRNA delivery material. Cyto-

toxicity analysis of 200 nM siRNA delivery by nanoparticles preparation (column 2), lipofectamine 2000 (column 3) and control cells (column 1) from left to right. Control cells represent cells untreated with siRNA. **d** Cytotoxicity exerted by the presence of antibiotics during transfection. Antibiotics cytotoxicity analysis of 200 nM siRNA delivery by nanoparticles preparation (column 2), lipofectamine 2000 (column 3) and control cells (column 1) from left to right. Control cells represent untreated with siRNA but treated with antibiotics

even at high concentration. Further study on utilization of antibiotic during transfection showed 10–15% of cell death (Fig. 5d, column 2) in nanotransfected cell compared to untransfected cells. But, this may be in acceptable range when we compared cell death occurred in lipofectamine 2000 transfection. Antibiotics caused approximately 40–50% cell death in cells transfected siRNA with Lipofectamine 2000 which is approximately 30–35% more than nanotransfection of siRNA (Fig. 5d column 3).

Efficacy of siRNA Loaded rec. Ctd Nanoparticles.

SupT1 cells were seeded in two sets. One set of cells were transfected with siRNA specific to Topo II β using nanoparticles and other set with Lipofectamine 2000. In both treatments equal amount of siRNA (~200 ng) was used. After treatment each set was divided into four parts and incubated. One part from both sets was collected at mentioned time periods, cells were lysed and Topo II β protein levels were studied from total protein by western blot. The Topo II β protein levels represent the knockdown efficiency of each transfecting method. Protein levels in nano-formulated siRNA-treated cells (Fig. 6a) were decreased

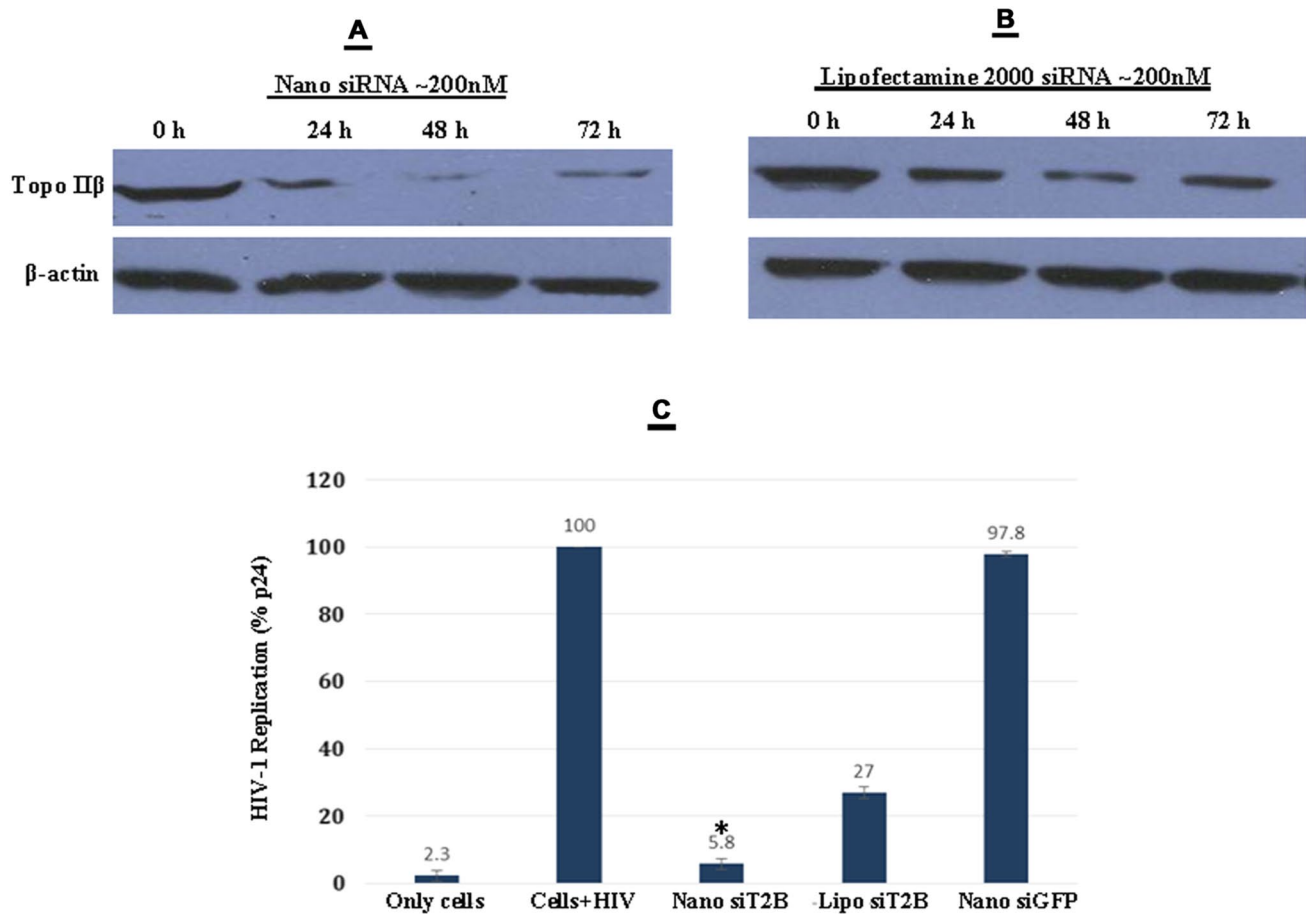


Fig. 6 Topoisomerase II β knockdown efficiency and effect on the HIV-1 replication. **a** Topo II β protein levels after nano-siRNA treatment. Protein levels were analyzed by western blot at 0 hpt, 24 hpt, 48 hpt and 72 hpt by keeping β -actin as a loading control. **b** Topo II β protein levels after lipofectamine 2000 mediated siRNA transfection. Protein levels were analyzed as mentioned above. In both experiment 0 h of post siRNA-treated samples used as control. **c** Effect of Topo II β knockdown on viral replication. After 48 hpt with nano-siRNA and Lipo siRNA, cells were infected with HIV-1. On third day the p24 present in the viral culture supernatants were estimated and plot-

ted. From left to right, Only cells: cells without infection but treated with 200 nM Topo II β siRNA, Cells+HIV: cells with infection but untreated with 200 nM Topo II β siRNA, Nano si T2B: cells treated with 200 nM Topo II β siRNA in the form of nanoparticles and infected with HIV-1, Lipo siT2B: cells treated with 200 nM Topo II β siRNA with lipofectamine 2000 and infected with HIV-1, Nano siGFP: cells treated with 200 nM GFP siRNA in the form of nanoparticles and infected with HIV-1. In this experiment, only cells used as negative control, Cells+HIV used as positive control and si RNA specific to GFP was used as siRNA control

considerably by 24 h of post-transfection (hpt) in comparison with 0 hpt and the levels were further decreased by 48 hpt and reached minimum. At 72 hpt the protein levels were slightly increased in comparison to 48 hpt. In case of transfection using Lipofectamine 2000 also (Fig. 6b), the protein levels followed the same pattern as like in nanotransfection. The comparison between each time point of different treatments makes lot of sense. At all time points, in nano-siRNA-treated cells less amount of Topo II β protein was observed than lipofectamine 2000 siRNA-treated cells. At 48 hpt the amount of protein in nano-siRNA-treated cells reached to almost zero (Fig. 6a). But, such a great decrease in protein levels were not observed in lipofectamine siRNA treatment (Fig. 6b). Moreover fast

recovery of protein levels in lipofectamine-treated cells was observed at 72 hpt than nano-siRNA-treated cells (Fig. 6b). These results clearly demonstrate siRNA transfection using nanoparticles knockdowns the target gene much more effectively than standard lipofectamine 2000.

Comparison of Viral Replication in Nano-siRNA and Lipofectamine-Mediated siRNA Transfection

SupT1 cells were divided into 5 parts and two parts were transfected with Topo II β specific and green fluorescent protein (GFP) specific siRNA in the form of nanoparticles separately. One part of cells were transfected with Topo II β specific siRNA using standard Lipofectamine 2000 and

remaining two parts were untreated. After 48 h of post incubation, except one untreated part, remaining four parts of cells were challenged with HIV-1 and the viral replication was measured 96 h later. The OD reading obtained from untreated and infected cells was taken as 100% of viral replication. Based on this the readings obtained in different treatments were calculated and represented in percent. Results show that (Fig. 6c) the standard lipofectamine siRNA-treated cells has supported 27% of viral replication (column 4 of Fig. 6c.). In nano-siRNA-treated cells, Topo II β specific siRNA supported only 5.8% of viral replication (column 3 of Fig. 6c) where as siRNA specific to GFP treatment supported 98% of viral replication (column 5 of Fig. 6c). The difference between virus production in siRNA untreated and siRNA GFP treated is not significant. But the viral production between siRNA Topo II β and siRNA GFP or siRNA untreated was significant. There was a significant difference between viral production in cells treated with nano-siRNA Topo II β and lipofectamine siRNA Topo II β . In nanodelivery system the viral replication was significantly decreased to nearly fourfold than lipofectamine delivery.

Discussion

In viral infected cells, the expression levels of transferrin receptor (Tfr) are highly unstable. In HIV-1 infection also, the cell surface Tfr levels upregulates up to 4 hpi, and at later stages it may undergo either downregulation or maintains the levels up to 20 hpi [39]. Our studies on Tfr also showed elevated levels at 4 hpi and reached normal level at 12 hpi and further decreased less than normal level at 24 hpi (Fig. 1a) highlighted possible targeted delivery to restrict early HIV-1 infection condition.

Transferrin (Tf) is the ligand for Tfr and Tf in the form of nanoparticles can also participate in receptor-ligand interactions [40]. The structure of Tf comprises two lobes called n-ter lobe and c-ter lobe connected by a small spacer peptide [41]. Out of these two, the c-ter lobe is sufficient for receptor binding and internalization [34].

To prepare protein nanoparticles using c-ter lobe of apotransferrin, the c-ter region from the ORF of apotransferrin mRNA was cloned (Fig. 1). The protein was over expressed (Fig. 2a, b), purified (Fig. 2c, d, e) and nanoparticles were prepared with either Doxorubicin Hcl (doxo) or siRNA. To evaluate the size and shape and drug delivering capacity of these nanoparticles, doxo c-ter nanoparticles were used. From the results it is evident that c-ter Tf nanoparticles were smaller in dimensions (~20–30 nm) (Fig. 3a) than the Tf nano which are in a size range of 60–80 nm (Fig. 3b), as reported earlier [37, 42]. From our results we identified a correlation between the size of the protein and

size of the nanoparticles. Decrease of one fold in molecular weight resulted in the twofold smaller nanoparticles and quantitatively the smaller nanoparticles are holding nearly 72% of the (Fig. 3c) drug input. During the functional assessment, like the Tf nanoparticles [43, 44], c-ter nanoparticles also showed a stable and prolonged release of the drug at around pH 5.5 was observed (Fig. 3d). Which indirectly shows the c-ter lobe retained the pH-dependent structure changing nature of transferrin. This nature was further confirmed by nanoparticle mediated drug delivery to HeLa cells. HeLa cells are the one of the cell types where transferrin and transferrin receptor mechanism of iron delivery was well studied [45, 46]. In vitro study in these cells showed the receptor targeted delivery of c-ter nanoformulation as efficient (Fig. 4b) as Tf nanoformulation. This could be due to the presence of the functional epitope which can bind to the Tfr [34, 47–49].

Targeting host or viral factors by siRNA to control infection is one of the method which is under developing [30]. Delivering effective quantities of siRNAs to the target remained as a major challenge [29]. To address this, we attempted to prepare siRNA loaded c-ter Tf nanoparticles and analyzed (Fig. 5a). These nanoparticles could able to accommodated majority (up to 80%) of the input siRNA (Fig. 5b) and with less cytotoxic effects than the standard transfecting agent (Fig. 5c). The additional advantage of these nanoparticles were having protection against antibiotic cytotoxicity (Fig. 5d) during transfection which could be due to the receptor mediated internalization of the nanoparticles. Lack of damage to plasma membrane prevented the antibiotic entry to the cell may be a possible reason for less cytotoxicity. This nature of the siRNA nanodelivery may increase the flexibility of *in vivo* siRNA delivery in the presence of antibiotic.

Topo II β knockdown has negative effects on HIV-1 replication which resulted in decreased viral progeny. Topo II β specific siRNA loaded c-ter nanoparticles were prepared and tested. Results showed the nanoparticles mediated delivery has advantage over lipofectamine (Fig. 6a). At 48 hpt, protein expression in nanotransfected cells was negligible compared to lipofectamine transfection (Fig. 6b). Even though, protein levels were increasing at 76 hpi in both conditions, but slowly in nanomediated transfection. The possible reason could be the availability of siRNA for longer periods providing prolonged knockdown effect or maybe because of slow and steady release of siRNA from nanoparticles provide longer availability of siRNA in the cell leads to the degradation of target mRNA may resulted in the slow raise in Topo II β protein level.

Available reports suggests that HIV-1 infection may enhance the protein levels of Topo II isoforms, especially Topo II β [28, 50]. Topo II β deficiency or prolonged low levels may abolish reverse transcription of HIV-1 genome

[28]. These siRNA loaded c-ter nanoparticles were tested against HIV-1 replication and found approximately five fold decrease in viral replication (Fig. 6c). This decreased viral load supported our hypothesis of using Tfr as a receptor for nanoparticle mediated deliver of antiviral agents to target very early events of HIV-1 infection cycle.

From this study we may conclude that Tfr-Tf system of delivery may be considered in strategies of targeting early HIV-1 infection to control the viral replication. Utilization of c-ter domain in the preparation of nanoparticles generate three times more drug holding capacity in half of the size increases efficiency of the nanoparticles. C-ter nanoparticles can be used for the delivery of either drug or siRNA.

Acknowledgements We thank the Council of Scientific and Industrial Research, India for providing doctoral fellowships to SLBK, Grants-in-Aid from Department of Science and Technology (DST), India to AKK supported this work completely. Infrastructure for this work is provided under University Grants Commission (UGC)-XI plan and Department of Biotechnology (DBT)-Centre for Research and Education in Biology and Biotechnology (CREBB) program of University of Hyderabad (UoH). We are grateful to Dr. J. Hoxie and Dr. R. Bollinger, NIH-AIDS reagent program, USA for kindly providing us with SupT1 cell line and HIV-1 93IN101 (subtype C). We thank Dr. K. Arun Kumar, Department of Animal Sciences, University of Hyderabad for providing us with HepG2 cell line.

Declarations

Conflict of interest Authors declare no conflict of interest.

References

- Osheroff, N. (1989). Biochemical basis for the interactions of type I and type II topoisomerases with DNA. *Pharmacology & Therapeutics*, 41(1–2), 223–241
- Zini, N., Martelli, A. M., Sabatelli, P., Santi, S., Negri, C., Astaldi Ricotti, G. C., & Maraldi, N. M. (1992). The 180-kDa isoform of topoisomerase II is localized in the nucleolus and belongs to the structural elements of the nucleolar remnant. *Experimental Cell Research*, 200(2), 460–466
- Capranico, G., Tinelli, S., Austin, C. A., Fisher, M. L., & Zunino, F. (1992). Different patterns of gene expression of topoisomerase II isoforms in differentiated tissues during murine development. *Biochimica et Biophysica Acta*, 1132(1), 43–48
- Yang, X., Li, W., Prescott, E. D., Burden, S. J., & Wang, J. C. (2000). DNA topoisomerase IIbeta and neural development. *Science*, 287(5450), 131–134
- Tsutsui, K., Tsutsui, K., Sano, K., Kikuchi, A., & Tokunaga, A. (2001). Involvement of DNA topoisomerase IIbeta in neuronal differentiation. *The Journal of Biological Chemistry*, 276(8), 5769–5778. <https://doi.org/10.1074/jbc.M008517200>
- Lyu, Y. L., & Wang, J. C. (2003). Aberrant lamination in the cerebral cortex of mouse embryos lacking DNA topoisomerase IIbeta. *Proceedings of the National Academy of Sciences of the United States of America*, 100(12), 7123–7128. <https://doi.org/10.1073/pnas.1232376100>
- Kaufmann, S. H., McLaughlin, S. J., Kastan, M. B., Liu, L. F., Karp, J. E., & Burke, P. J. (1991). Topoisomerase II levels during granulocytic maturation in vitro and in vivo. *Cancer Research*, 51(13), 3534–3543
- Kaufmann, S. H., Charron, M., Burke, P. J., & Karp, J. E. (1995). Changes in topoisomerase I levels and localization during myeloid maturation in vitro and in vivo. *Cancer Research*, 55(6), 1255–1260
- Aoyama, M., Grabowski, D. R., Isaacs, R. J., Krivacic, K. A., Rybicki, L. A., Bukowski, R. M., Ganapathi, M. K., Hickson, I. D., & Ganapathi, R. (1998). Altered expression and activity of topoisomerases during all-trans retinoic acid-induced differentiation of HL-60 cells. *Blood*, 92(8), 2863–2870
- Chikamori, K., Hill, J. E., Grabowski, D. R., Zarkhin, E., Grozav, A. G., Vaziri, S. A., Wang, J., Gudkov, A. V., Rybicki, L. R., Bukowski, R. M., Yen, A., Tanimoto, M., Ganapathi, M. K., & Ganapathi, R. (2006). Downregulation of topoisomerase IIbeta in myeloid leukemia cell lines leads to activation of apoptosis following all-trans retinoic acid-induced differentiation/growth arrest. *Leukemia*, 20(10), 1809–1818. <https://doi.org/10.1038/sj.leu.2404351>
- Cowell, I. G., Okorokov, A. L., Cutts, S. A., Padget, K., Bell, M., Milner, J., & Austin, C. A. (2000). Human topoisomerase IIalpha and IIbeta interact with the C-terminal region of p53. *Experimental Cell Research*, 255(1), 86–94. <https://doi.org/10.1006/excr.1999.4772>
- Bhat, U. G., Raychaudhuri, P., & Beck, W. T. (1999). Functional interaction between human topoisomerase IIalpha and retinoblastoma protein. *Proceedings of the National Academy of Sciences of the United States of America*, 96(14), 7859–7864
- Kroll, D. J., Sullivan, D. M., Gutierrez-Hartmann, A., & Hoeffler, J. P. (1993). Modification of DNA topoisomerase II activity via direct interactions with the cyclic adenosine-3',5'-monophosphate response element-binding protein and related transcription factors. *Molecular Endocrinology*, 7(3), 305–318. <https://doi.org/10.1210/mend.7.3.8387155>
- Tsai, S. C., Valkov, N., Yang, W. M., Gump, J., Sullivan, D., & Seto, E. (2000). Histone deacetylase interacts directly with DNA topoisomerase II. *Nature Genetics*, 26(3), 349–353. <https://doi.org/10.1038/81671>
- Johnson, C. A., Padget, K., Austin, C. A., & Turner, B. M. (2001). Deacetylase activity associates with topoisomerase II and is necessary for etoposide-induced apoptosis. *The Journal of Biological Chemistry*, 276(7), 4539–4542. <https://doi.org/10.1074/jbc.C000824200>
- Kurz, E. U., Leader, K. B., Kroll, D. J., Clark, M., & Gieseler, F. (2000). Modulation of human DNA topoisomerase IIalpha function by interaction with 14-3-3epsilon. *The Journal of Biological Chemistry*, 275(18), 13948–13954
- Durrieu, F., Samejima, K., Fortune, J. M., Kandels-Lewis, S., Osheroff, N., & Earnshaw, W. C. (2000). DNA topoisomerase IIalpha interacts with CAD nuclease and is involved in chromatin condensation during apoptotic execution. *Current Biology*, 10(15), 923–926
- Barker, C. R., Hamlett, J., Pennington, S. R., Burrows, F., Lundgren, K., Lough, R., Watson, A. J., & Jenkins, J. R. (2006). The topoisomerase II-Hsp90 complex: A new chemotherapeutic target? *International Journal of Cancer*, 118(11), 2685–2693. <https://doi.org/10.1002/ijc.21717>
- Wong, M. L., & Hsu, M. T. (1990). Involvement of topoisomerases in replication, transcription, and packaging of the linear adenovirus genome. *Journal of Virology*, 64(2), 691–699
- Lin, Y. C., Li, J., Irwin, C. R., Jenkins, H., DeLange, L., & Evans, D. H. (2008). Vaccinia virus DNA ligase recruits cellular topoisomerase II to sites of viral replication and assembly. *Journal of Virology*, 82(12), 5922–5932. <https://doi.org/10.1128/JVI.02723-07>

21. Cereseto, A., & Giacca, M. (2004). Integration site selection by retroviruses. *AIDS Reviews*, 6(1), 13–21
22. Schmidt, B., Ashlock, B. M., Foster, H., Fujimura, S. H., & Levy, J. A. (2005). HIV-infected cells are major inducers of plasmacytoid dendritic cell interferon production, maturation, and migration. *Virology*, 343(2), 256–266. <https://doi.org/10.1016/j.virol.2005.09.059>
23. Benson, J. D., & Huang, E. S. (1988). Two specific topoisomerase II inhibitors prevent replication of human cytomegalovirus DNA: An implied role in replication of the viral genome. *Journal of Virology*, 62(12), 4797–4800
24. Huang, E. S., Benson, J. D., Huong, S. M., Wilson, B., & van der Horst, C. (1992). Irreversible inhibition of human cytomegalovirus replication by topoisomerase II inhibitor, etoposide: A new strategy for the treatment of human cytomegalovirus infection. *Antiviral Research*, 17(1), 17–32
25. Bouille, P., Subra, F., Mouscadet, J. F., & Auclair, C. (1999). Antisense-mediated repression of DNA topoisomerase II expression leads to an impairment of HIV-1 replicative cycle. *Journal of Molecular Biology*, 285(3), 945–954. <https://doi.org/10.1006/jmbi.1998.2360>
26. Matthes, E., Langen, P., Brachwitz, H., Schroder, H. C., Maidhof, A., Weiler, B. E., Renneisen, K., & Muller, W. E. (1990). Alteration of DNA topoisomerase II activity during infection of H9 cells by human immunodeficiency virus type 1 in vitro: A target for potential therapeutic agents. *Antiviral Research*, 13(6), 273–286
27. Kondapi, A. K., Satyanarayana, N., & Saikrishna, A. D. (2006). A study of the topoisomerase II activity in HIV-1 replication using the ferrocene derivatives as probes. *Archives of Biochemistry and Biophysics*, 450(2), 123–132. <https://doi.org/10.1016/j.abb.2006.04.003>
28. Lokeswara Balakrishna, S., Satyanarayana, N., & Kondapi, A. K. (2013). Involvement of human topoisomerase II isoforms in HIV-1 reverse transcription. *Archives of Biochemistry and Biophysics*, 532(2), 91–102. <https://doi.org/10.1016/j.abb.2013.01.010>
29. Kirchhoff, F. (2008). Silencing HIV-1 In Vivo. *Cell*, 134(4), 566–568. <https://doi.org/10.1016/j.cell.2008.08.004>
30. Boden, D., Pusch, O., & Ramratnam, B. (2004). HIV-1-specific RNA interference. *Current Opinion in Molecular Therapeutics*, 6(4), 373–380
31. Qian, Z. M., Li, H., Sun, H., & Ho, K. (2002). Targeted drug delivery via the transferrin receptor-mediated endocytosis pathway. *Pharmacological Reviews*, 54(4), 561–587
32. Aisen, P. (1998). Transferrin, the transferrin receptor, and the uptake of iron by cells. *Metal Ions in Biological Systems*, 35, 585–631
33. Hemadi, M., Kahn, P. H., Miquel, G., & El HageChahine, J. M. (2004). Transferrin's mechanism of interaction with receptor 1. *Biochemistry*, 43(6), 1736–1745. <https://doi.org/10.1021/bi030142g>
34. Zak, O., Trinder, D., & Aisen, P. (1994). Primary receptor-recognition site of human transferrin is in the C-terminal lobe. *The Journal of Biological Chemistry*, 269(10), 7110–7114
35. Smith, S. D., Shatsky, M., Cohen, P. S., Warnke, R., Link, M. P., & Glader, B. E. (1984). Monoclonal antibody and enzymatic profiles of human malignant T-lymphoid cells and derived cell lines. *Cancer Research*, 44(12 Pt 1), 5657–5660
36. Mandraju, R. K., Kannapiran, P., & Kondapi, A. K. (2008). Distinct roles of topoisomerase II isoforms: DNA damage accelerating alpha, double strand break repair promoting beta. *Archives of Biochemistry and Biophysics*, 470(1), 27–34. <https://doi.org/10.1016/j.abb.2007.10.017>
37. Krishna, A. D., Mandraju, R. K., Kishore, G., & Kondapi, A. K. (2009). An efficient targeted drug delivery through apotransferrin loaded nanoparticles. *PLoS ONE*, 4(10), e7240. <https://doi.org/10.1371/journal.pone.0007240>
38. Towbin, H., Staehelin, T., & Gordon, J. (1979). Electrophoretic transfer of proteins from polyacrylamide gels to nitrocellulose sheets: Procedure and some applications. *Proceedings of the National Academy of Sciences of the United States of America*, 76(9), 4350–4354
39. Navare, A. T., Sova, P., Purdy, D. E., Weiss, J. M., Wolf-Yadlin, A., Korth, M. J., Chang, S. T., Proll, S. C., Jahan, T. A., Krasnoselsky, A. L., Palermo, R. E., & Katze, M. G. (2012). Quantitative proteomic analysis of HIV-1 infected CD4+ T cells reveals an early host response in important biological pathways: Protein synthesis, cell proliferation, and T-cell activation. *Virology*, 429(1), 37–46. <https://doi.org/10.1016/j.virol.2012.03.026>
40. Gandapu, U., Chaitanya, R. K., Kishore, G., Reddy, R. C., & Kondapi, A. K. (2011). Curcumin-loaded apotransferrin nanoparticles provide efficient cellular uptake and effectively inhibit HIV-1 replication in vitro. *PLoS ONE*, 6(8), e23388. <https://doi.org/10.1371/journal.pone.0023388>
41. MacGillivray, R. T., Mendez, E., Shewale, J. G., Sinha, S. K., Lineback-Zins, J., & Brew, K. (1983). The primary structure of human serum transferrin. The structures of seven cyanogen bromide fragments and the assembly of the complete structure. *The Journal of Biological Chemistry*, 258(6), 3543–3553
42. Golla, K., Cherukuvada, B., Ahmed, F., & Kondapi, A. K. (2012). Efficacy, safety and anticancer activity of protein nanoparticle-based delivery of doxorubicin through intravenous administration in rats. *PLoS ONE*, 7(12), e51960. <https://doi.org/10.1371/journal.pone.0051960>
43. Golla, K., Bhaskar, C., Ahmed, F., & Kondapi, A. K. (2013). A target-specific oral formulation of Doxorubicin-protein nanoparticles: Efficacy and safety in hepatocellular cancer. *Journal of Cancer*, 4(8), 644–652. <https://doi.org/10.7150/jca.7093>
44. Golla, K., Reddy, P. S., Bhaskar, C., & Kondapi, A. K. (2013). Biocompatibility, absorption and safety of protein nanoparticle-based delivery of doxorubicin through oral administration in rats. *Drug Delivery*, 20(3–4), 156–167. <https://doi.org/10.3109/10717544.2013.801051>
45. Lamb, J. E., Ray, F., Ward, J. H., Kushner, J. P., & Kaplan, J. (1983). Internalization and subcellular localization of transferrin and transferrin receptors in HeLa cells. *The Journal of Biological Chemistry*, 258(14), 8751–8758
46. Bleil, J. D., & Bretscher, M. S. (1982). Transferrin receptor and its recycling in HeLa cells. *The EMBO Journal*, 1(3), 351–355
47. Zak, O., & Aisen, P. (2002). A new method for obtaining human transferrin C-lobe in the native conformation: Preparation and properties. *Biochemistry*, 41(5), 1647–1653
48. Giannetti, A. M., Snow, P. M., Zak, O., & Bjorkman, P. J. (2003). Mechanism for multiple ligand recognition by the human transferrin receptor. *PLoS Biology*, 1(3), E51. <https://doi.org/10.1371/journal.pbio.0000051>
49. Thorstensen, K., Trinder, D., Zak, O., & Aisen, P. (1995). Uptake of iron from N-terminal half-transferrin by isolated rat hepatocytes. Evidence of transferrin-receptor-independent iron uptake. *European Journal of Biochemistry*, 232(1), 129–133
50. Mandraju, R. K., & Kondapi, A. K. (2007). Regulation of topoisomerase II alpha and beta in HIV-1 infected and uninfected neuroblastoma and astrocytoma cells: Involvement of distinct norehydroguaretic acid sensitive inflammatory pathways. *Archives of Biochemistry and Biophysics*, 461(1), 40–49. <https://doi.org/10.1016/j.abb.2007.01.026>